

Available online at www.sciencedirect.com**ScienceDirect**

Geochimica et Cosmochimica Acta 226 (2018) 192–205

**Geochimica et
Cosmochimica
Acta**

www.elsevier.com/locate/gca

Mg isotope systematics during magmatic processes: Inter-mineral fractionation in mafic to ultramafic Hawaiian xenoliths

A. Stracke^{a,b,*}, E.T. Tipper^{a,c}, S. Klemme^b, M. Bizimis^d^a *Institute of Isotope Geochemistry and Mineral Resources, ETH Zurich, Clausiusstrasse 25, 8092 Zurich, Switzerland*^b *Institut für Mineralogie, Westfälische Wilhelms-Universität, Corrensstrasse 24, 48149 Münster, Germany*^c *Department of Earth Sciences, University of Cambridge, Downing Street, Cambridge CB2 3EQ, UK*^d *School of Earth, Ocean, and Environment, University of South Carolina, 701 Sumter St., EWSC 617, Columbia, SC 29208 USA*

Received 2 May 2017; accepted in revised form 2 February 2018; available online 12 February 2018

Abstract

Observed differences in Mg isotope ratios between bulk magmatic rocks are small, often on a sub per mill level. Inter-mineral differences in the $^{26}\text{Mg}/^{24}\text{Mg}$ ratio (expressed as $\delta^{26}\text{Mg}$) in plutonic rocks are on a similar scale, and have mostly been attributed to equilibrium isotope fractionation at magmatic temperatures. Here we report Mg isotope data on minerals in spinel peridotite and garnet pyroxenite xenoliths from the rejuvenated stage of volcanism on Oahu and Kauai, Hawaii. The new data are compared to literature data and to theoretical predictions to investigate the processes responsible for inter-mineral Mg isotope fractionation at magmatic temperatures. Theory predicts up to per mill level differences in $\delta^{26}\text{Mg}$ between olivine and spinel at magmatic temperatures and a general decrease in $\Delta^{26}\text{Mg}_{\text{olivine-spinel}}$ ($=\delta^{26}\text{Mg}_{\text{olivine}} - \delta^{26}\text{Mg}_{\text{spinel}}$) with increasing temperature, but also with increasing Cr# in spinel. For peridotites with a simple petrogenetic history by melt depletion, where increasing depletion relates to increasing melting temperatures, $\Delta^{26}\text{Mg}_{\text{olivine-spinel}}$ should thus systematically decrease with increasing Cr# in spinel. However, most natural peridotites, including the Hawaiian spinel peridotites investigated in this study, are overprinted by variable extents of melt-rock reaction, which disturb the systematic primary temperature and compositionally related olivine–spinel Mg isotope systematics. Diffusion, subsolidus re-equilibration, or surface alteration may further affect the observed olivine–spinel Mg isotope fractionation in peridotites, making $\Delta^{26}\text{Mg}_{\text{olivine-spinel}}$ in peridotites a difficult-to-apply geothermometer. The available Mg isotope data on clinopyroxene and garnet suggest that this mineral pair is a more promising geothermometer, but its application is restricted to garnet-bearing igneous (garnet pyroxenites) and metamorphic rocks (eclogites). Although the observed $\delta^{26}\text{Mg}$ variation is on a sub per mill range in bulk magmatic rocks, the clearly resolvable inter-mineral Mg isotope differences imply that crystallization or preferential melting of isotopically distinct minerals such as garnet, spinel, and clinopyroxene should cause Mg isotope fractionation between bulk melt and residue. Calculated Mg isotope variations during partial mantle melting indeed predict differences between melt and residue, but these are analytically resolvable only for melting of mafic lithologies, that is, garnet pyroxenites. Contributions from garnet pyroxenite melts may thus account for some of the isotopically light $\delta^{26}\text{Mg}$ observed in ocean island basalts

* Corresponding author at: Institut für Mineralogie, Westfälische Wilhelms-Universität, Corrensstrasse 24, 48149 Münster, Germany.
E-mail address: stracke.andreas@uni-muenster.de (A. Stracke).

and trace lithological mantle heterogeneity. Consequently, applications for high-temperature Mg isotope fractionations are promising and diverse, and recent advances in analytical precision may allow the full petrogenetic potential inherent in the sub per mill variations in $\delta^{26}\text{Mg}$ in magmatic rocks to be exploited.

© 2018 Elsevier Ltd. All rights reserved.

Keywords: Mg isotopes; Peridotite; Bulk earth; Mantle; Basalt

1. INTRODUCTION

Over the past 15 years, variations in Mg isotope ratios have become an important tool for investigating Mg cycling in Earth's surface environments. Early research focused on low temperature processes because of the associated large (ca. 5‰) Mg isotope variation (e.g., Galy et al., 2002; Young and Galy, 2004; Tipper et al., 2006a; 2006b; 2006c; Brenot et al., 2008; Pogge von Strandmann et al., 2008a; 2008b; Tipper et al., 2008a; Hippler et al., 2009; Shen et al., 2009; Teng et al., 2010b).

Recently, there is a growing body of work on Mg isotopes at high temperature, sparked by the expectation that isotope ratios of Mg—the second most abundant element in the bulk silicate earth—directly mirror planetary compositions and trace global (bio)geochemical cycles. It has been shown, for example, that there is broad overlap between different types of chondrites, lunar and martian rocks (Young and Galy, 2004; Norman et al., 2006; Wiechert and Halliday, 2007; Handler et al., 2009; Bourdon et al., 2010; Schiller et al., 2010; Teng et al., 2010a; Pogge von Strandmann et al., 2011; Sedaghatpour et al., 2013). The Earth's mantle contains ca. 99.9% of Earth's Mg. Its average Mg isotope ratio is thus representative of the bulk earth and is similar to those of meteorites (Handler et al., 2009; Yang et al., 2009; Bourdon et al., 2010; Dauphas et al., 2010; Schiller et al., 2010; Teng et al., 2010a; Bizzarro et al., 2011; Huang et al., 2011; Liu et al., 2011; Pogge von Strandmann et al., 2011; Xiao et al., 2013). Hence Mg isotope fractionation during planetary accretion and differentiation is difficult to resolve. The average Mg isotope composition of Earth's mantle (peridotite) and its derivative melts (MORB and OIB) is identical (Teng et al., 2007; Bourdon et al., 2010; Teng et al., 2010a; Dauphas et al., 2010; Huang et al., 2011). Most previous studies have therefore concluded that there is no clearly resolvable Mg isotope fractionation on a bulk sample scale during mantle melting and melt differentiation, which contrasts with observations from other major elements such as Fe (Weyer and Ionov, 2007; Teng et al., 2013; Williams and Bizimis, 2014).

In contrast, recent studies have documented clearly resolvable Mg isotope fractionation between minerals in mantle peridotites (e.g., Wiechert and Halliday, 2007; Handler et al., 2009; Yang et al., 2009; Young et al., 2009; Huang et al., 2011; Li et al., 2011; Liu et al., 2011; Pogge von Strandmann et al., 2011; Wang et al., 2012; Xiao et al., 2013; Hu et al., 2016; Wang et al., 2016). These inter-mineral Mg isotope differences in mantle peridotites (and eclogites) are generally thought to reflect equilibrium magmatic fractionation, but in some cases were attributed

to metasomatism (Young et al., 2009; Huang et al., 2011; Xiao et al., 2013; Hu et al., 2016), or to diffusion (e.g., Huang et al., 2011; Pogge von Strandmann et al., 2011; Sio et al., 2013; Oeser et al., 2015). Here we report Mg isotope data on minerals in spinel peridotite and garnet pyroxenite xenoliths from the rejuvenated stage of volcanism on Oahu and Kauai, Hawaii. The new data are compared to literature data and to theoretical predictions to investigate the processes responsible for inter-mineral Mg isotope fractionation at magmatic temperatures, with a special focus on the relative roles of temperature and composition. In light of the observed inter-mineral Mg isotope differences, it would be expected that partial mantle melting, which preferentially consumes the isotopically distinct phases clinopyroxene and garnet, may lead to resolvable differences between melt (basalt) and residue (peridotite). Indeed, Zhong et al. (2017) recently suggested that small, <0.2‰, differences in $\delta^{26}\text{Mg}$ occur during partial mantle melting, but the magnitude of this fractionation relies on the inferred isotope fractionation factor between residual source (peridotite or garnet pyroxenite) and melt. Here, we present a general model for partial melting that accounts for isotopic changes in melt composition due to variable contribution of isotopically diverse minerals to the melt. We show that partial melting of mantle peridotite does not generate resolvable Mg isotope fractionation, consistent with the general overlap in $\delta^{26}\text{Mg}$ between peridotite and basalt (Teng et al., 2007; Bourdon et al., 2010; Dauphas et al., 2010; Teng et al., 2010a; Huang et al., 2011). In contrast, melting of garnet-bearing mafic source lithologies (garnet pyroxenites) produces larger Mg isotope fractionation between source and melt. In the absence of experimentally determined mineral–melt isotope fractionation factors, however, the overall offset between bulk melt and residual rock remains uncertain, but low $\delta^{26}\text{Mg}$ at high Sm/Yb observed in some ocean island basalts hint at a possible signature of garnet pyroxenite melting, and may thus trace lithological mantle heterogeneity.

2. SAMPLES AND ANALYTICAL TECHNIQUES

2.1. Sample selection and systematics

Five spinel peridotite and five garnet pyroxenite xenoliths from two locations on the Hawaiian islands were analyzed. All xenoliths are found within the rejuvenated stage alkali lavas from Oahu (Honolulu Volcanics (Clague and Frey, 1982)) and Kauai, Hawaii (Koloa volcanics (Garcia et al., 2010)). Samples labeled 77SL-x or Pa-x are from the Presnal collection, the 114954-x pyroxenites are from the Jackson collection, both housed at the Smithsonian

Table 1
Mg isotope data for the Hawaiian spinel peridotites and garnet pyroxenites.

Sample	Mineral	$\delta^{26}\text{Mg}$	2 S.D.	$\delta^{25}\text{Mg}$	2 S.D.	$\Delta^{25}\text{Mg}'$
<i>Spinel peridotites</i>						
07Han001	ol	−0.21	0.02	−0.1	0.03	0.005
07Han001	cpx	−0.16	0.01	−0.07	0.03	0.008
07Han001	sp	0.07	0.04	0.05	0.01	0.015
Pa27	ol	−0.24	0.04	−0.12	0.02	0.001
Pa27	opx	−0.22	0.06	−0.11	0.03	−0.001
Pa27	cpx	−0.32	0.03	−0.17	0.04	−0.001
Pa27	sp	−0.03	0.16	0	0.07	0.009
77SL405	ol	−0.17	0.07	−0.08	0.02	0.006
77SL405	opx	−0.16	0.1	−0.09	0.03	−0.009
77SL405	cpx	−0.13	0.11	−0.07	0.04	−0.003
77SL466	ol	−0.2	0.03	−0.11	0.06	−0.003
77SL466	opx	−0.2	0.05	−0.12	0.04	−0.009
77SL466	cpx	−0.15	0.1	−0.08	0.06	−0.001
77SL466	sp	0.04	0.03	0.02	0.03	0
77SL470	ol	−0.22	0.04	−0.11	0.02	0.005
77SL470	opx	−0.15	0.06	−0.09	0.02	−0.012
77SL470	cpx	−0.11	0.02	−0.06	0.01	0.001
<i>Garnet pyroxenites</i>						
77SL582	cpx	−0.1	0.03	−0.05	0.04	−0.001
77SL582	grt	−0.52	0.07	−0.27	0.06	−0.001
77SL620	cpx	0	0.19	0	0.08	−0.004
77SL620	grt	−0.38	0.09	−0.2	0.02	−0.004
77SL744	cpx	0.02	0.08	0.01	0.02	−0.005
77SL744	grt	−0.39	0.03	−0.21	0.03	−0.008
114954-20A	cpx	−0.03	0.06	−0.01	0.02	0.003
114954-20A	grt	−0.42	0.04	−0.21	0.04	0.005
114954-28A	cpx	−0.13	0.02	−0.05	0.04	0.014
114954-28A	grt	−0.58	0.03	−0.29	0.01	0.008

$\Delta^{25}\text{Mg}' = \delta^{25}\text{Mg}' - 0.521 * \delta^{26}\text{Mg}'$, with $\delta^{2x}\text{Mg}' = 1000 * \ln((\delta^{2x}\text{Mg} + 1000)/1000)$ (Young and Galy, 2004).

Institution, Washington (Table 1). The 07Hana-001 peridotite is from the Hanapepe location, Kauai, Hawaii. The 77SL-x samples are exceptionally fresh, while the olivines in the 007Hana-001 and Pa27 samples show minor signs of alteration. Only the cleanest minerals, free of inclusions or blemishes, were handpicked for the Mg isotope analyses.

Major, trace element, and Hf, Nd, Sr, and Os isotopes compositions of the spinel peridotites from the Salt Lake Crater (SLC) and Pali vents in Oahu have been reported by Bizimis et al. (2004; 2007), and by a series of publications for the garnet pyroxenites (Keshav and Sen, 2001; Bizimis et al., 2005; Keshav et al., 2007; Sen et al., 2010; 2011; Bizimis et al., 2013). The peridotites are either fragments of the in-situ Pacific mantle lithosphere (Sen et al., 2005), or ancient recycled oceanic lithospheric components of the plume Hawaiian source (Bizimis et al., 2007). The garnet pyroxenite xenoliths are interpreted as high-pressure (2–3 GPa) cumulates from melts erupted during the rejuvenated phase of volcanism (Bizimis et al., 2005; Sen et al., 2005). Further details on the composition and origin of the analyzed samples are discussed in the supplementary information 1. In summary, the selected Hawaiian peridotites cover almost the entire range of depletions observed

in abyssal peridotites and have a wide range of isotope and trace element compositions. Hence, they are ideally suited for investigating whether there is a compositional effect on inter-mineral Mg isotope fractionation at magmatic P–T conditions. In addition, the selected garnet pyroxenites provide a unique opportunity to investigate Mg isotope variability in non-peridotitic lithologies of the oceanic mantle, and for evaluating the Mg isotope fractionation between clinopyroxene and garnet as a potential geothermometer (Huang et al., 2013).

2.2. Analytical techniques

The employed analytical techniques are identical to those described in detail in Tipper et al., (2008b) and Bourdon et al. (2010), but are summarized below.

Powdered mineral separates were digested in a 1:1 concentrated HF-HNO₃ mixture for a minimum of 24 h at ~150 °C, with the exception of the spinels, which were digested under high-pressure in Parr bombs in HF-HNO₃ for 3–4 days to ensure complete dissolution. Afterwards, sample solutions were dried down and redissolved in 6 N HCl, the latter step was repeated twice to eliminate any

remaining fluorides. An aliquot of these solutions containing 20 µg of Mg (<1% by weight) was evaporated and dissolved in 12 N HCl to be loaded on a 2 ml BioRad AG1-X8 anion column, Cl⁻ form, 200–400 mesh. Mg was eluted in 12 N HCl, and the Mg fraction was evaporated, redissolved in 0.4 N HCl and loaded onto a 1 ml cation exchange column (Biorad AG50W-X12). Mg was collected in 1 N HCl, and this column procedure was repeated to obtain a pure Mg fraction. The solutions were evaporated and heated to 170 °C in aqua regia for 24hrs before redissolving in 16 N HNO₃ to convert to a nitric salt, then evaporated, and dissolved in 2% HNO₃ at ~20 ppm, ready for final dilution immediately prior to analysis. Total procedural blanks were less than 10 ng (<0.05% of the total Mg processed).

Mg isotope ratios were measured on a Nu Plasma MC-ICPMS at IGMR, ETH Zurich, using an APEX Q sample introduction system coupled to an ESI ACM membrane. The samples were aspirated using a PFA nebulizer with nominal uptake of 20 µl/min, resulting in excess of 14 V total beam of Mg for a 200 ppb solution at an actual uptake of ca. 10 µl/min. Prior to introduction of the samples into the mass spectrometer, all solutions were centrifuged, and diluted to within 10% of the concentration of the DSM3 reference standard (200 ppb).

Measurements were made using a standard bracketing protocol identical to that of [Tipper et al. \(2008b\)](#). External reproducibility (precision) of mono-elemental standards over the 14-month period of analysis was 0.095‰ (2 S.D.) for δ²⁶Mg. Based on the total number of procedural replicate analyses of both mono-elemental and multi-elemental standards, the maximum 2 S.D. uncertainty was estimated as 0.094‰ for δ²⁶Mg and 0.052‰ for δ²⁵Mg ([Bourdon et al., 2010](#)).

3. RESULTS

Olivine (ol) and clinopyroxene (cpx) have been analyzed in all five spinel peridotites, orthopyroxene (opx) from four of the five peridotites, and isolated spinel (sp) grains suitable for Mg isotope analyses could be recovered from three peridotite samples. Garnet (grt) and cpx have been analyzed in all five pyroxenites ([Table 1, Fig. 1](#)).

In the peridotites, the δ²⁶Mg values of the olivine, orthopyroxene and clinopyroxene are similar ([Table 1 and Fig. 1](#)), with δ²⁶Mg_{ol} = -0.24 to -0.17‰, δ²⁶Mg_{opx} = -0.22 to -0.15‰, and δ²⁶Mg_{cpx}^{peridotite} = -0.32 to -0.11‰. The δ²⁶Mg values in the spinels range to more positive values with δ²⁶Mg_{sp} = -0.03 to +0.07. Although the δ²⁶Mg values in clinopyroxene from peridotites and pyroxenites overlap, the δ²⁶Mg_{cpx} in the pyroxenites range to more positive values with δ²⁶Mg_{cpx}^{pyroxenite} = -0.13 to +0.02. The garnets from the pyroxenites have overall the most negative δ²⁶Mg values ranging from -0.58 to -0.38‰.

Calculated bulk rock δ²⁶Mg values for the peridotites (δ²⁶Mg = -0.24 to -0.16) and pyroxenites (δ²⁶Mg = -0.26 to -0.08) are close to the average value calculated for mantle-derived rocks (peridotites and basalts: δ²⁶Mg = -0.244 ± 0.062, 2 S.D., [supplementary data; \(Wiechert and Halliday, 2007; Handler et al., 2009; Yang et al., 2009; Young et al., 2009; Huang et al., 2011; Li et al.,](#)

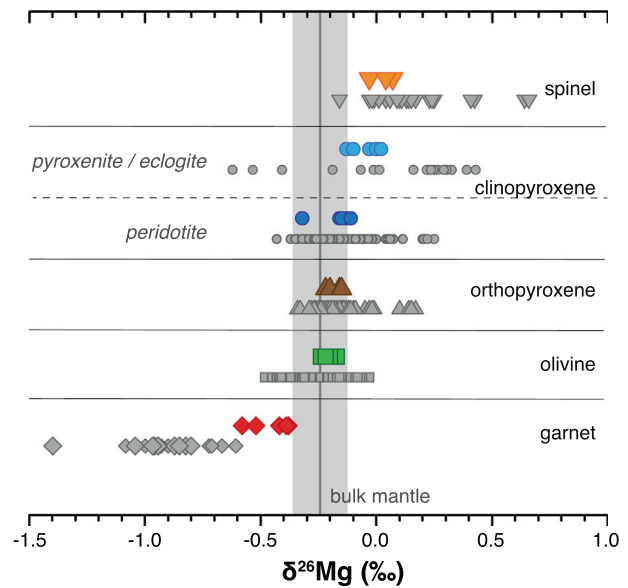


Fig. 1. δ²⁶Mg values in minerals from the Hawaiian spinel peridotite (olivine, orthopyroxene, clinopyroxene, spinel) and garnet pyroxenite (garnet, clinopyroxene) xenoliths investigated in this study (colored symbols) compared to δ²⁶Mg values in minerals from peridotites and eclogites reported in the literature (gray symbols). Literature data are from ([Wiechert and Halliday, 2007; Handler et al., 2009; Yang et al., 2009; Young et al., 2009; Huang et al., 2011; Li et al., 2011; Liu et al., 2011; Pogge von Strandmann et al., 2011; Wang et al., 2012; Xiao et al., 2013; Wang et al., 2014; Wang et al., 2016](#)). (For interpretation of the references to colour in this figure legend, the reader is referred to the web version of this article.)

[2011; Liu et al., 2011; Pogge von Strandmann et al., 2011; Wang et al., 2012; Xiao et al., 2013; Wang et al., 2014; Hu et al., 2016; Wang et al., 2016; Zhong et al., 2017](#)). In three-isotope plots of δ²⁵Mg' versus δ²⁶Mg' (δ^{2x}Mg' = 100 0 * ln((δ^{2x}Mg + 1000)/1000); ([Young and Galy, 2004](#))) the Hawaiian data define a line with a slope of 0.527 ± 0.087 (r² = 0.994), which is within error of the slope of 0.521 expected for equilibrium isotope fractionation ([Young and Galy, 2004](#)).

Inter-mineral fractionation factors for the peridotite minerals Δ²⁶Mg_{x-y}, calculated as δ²⁶Mg_x - δ²⁶Mg_y—where x and y are different mineral phases—show no resolvable Mg isotope fractionation between ol and opx (Δ²⁶Mg_{ol-opx} = -0.07 to 0; [Fig. 2](#)). δ²⁶Mg values in the clinopyroxenes, however, are slightly higher than those in ol or opx (e.g., Δ²⁶Mg_{ol-cpx} = -0.11 to +0.08). Clearly resolvable, and uniform inter-mineral fractionation is observed between the spinels and other peridotite minerals (e.g., Δ²⁶Mg_{ol-sp} = -0.28 to -0.21). These inter-mineral Mg isotope fractionations are within the range of previously reported values in peridotites: Δ²⁶Mg_{ol-opx} = -0.39 to +0.07, Δ²⁶Mg_{ol-cpx} = -0.42 to +0.08, and Δ²⁶Mg_{ol-sp} = -0.88 to -0.16 ([Fig. 2; \(Young et al., 2009; Liu et al., 2011; Xiao et al., 2013; Wang et al., 2016\)](#)). In the pyroxenites, δ²⁶Mg_{grt} is consistently lower than δ²⁶Mg_{cpx}^{pyroxenite}, by -0.45 to -0.38‰ (Δ²⁶Mg_{grt-cpx}). This is about a factor of 2.7 less than reported for metamorphic garnet-omphacite

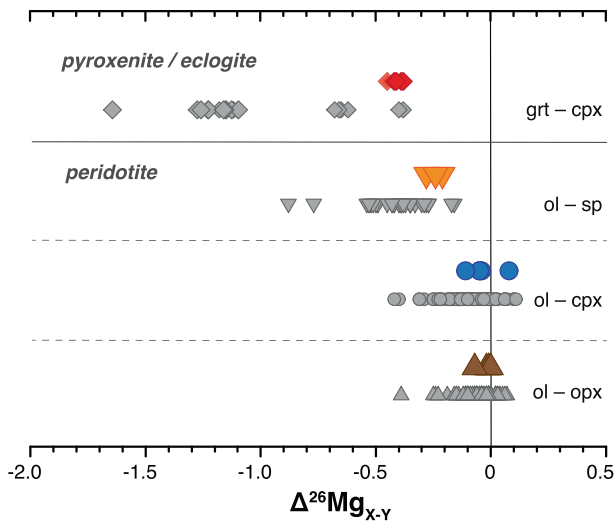


Fig. 2. Inter-mineral fractionation factors $\Delta^{26}\text{Mg}_{\text{X-Y}} = \delta^{26}\text{Mg}_{\text{X}} - \delta^{26}\text{Mg}_{\text{Y}}$ for minerals from Hawaiian spinel peridotites (olivine, orthopyroxene, clinopyroxene, spinel) and garnet pyroxenites (garnet, clinopyroxene) (colored symbols) compared to $\Delta^{26}\text{Mg}_{\text{X-Y}}$ values in minerals from spinel peridotites and eclogites reported in the literature (gray symbols). Literature data are from (Wiechert and Halliday, 2007; Handler et al., 2009; Yang et al., 2009; Young et al., 2009; Huang et al., 2011; Li et al., 2011; Liu et al., 2011; Pogge von Strandmann et al., 2011; Wang et al., 2012; Xiao et al., 2013; Wang et al., 2014; Wang et al., 2016). (For interpretation of the references to color in this figure legend, the reader is referred to the web version of this article.)

pairs ($\Delta^{26}\text{Mg}_{\text{grt-cpx}} = -1.65$ to -1.10) in eclogites reported by Li et al. (2011) and Wang et al. (2014) (Fig. 2), but within the range of values reported for eclogites from the South African subcontinental lithospheric mantle by Wang et al. (2012) ($\Delta^{26}\text{Mg}_{\text{grt-cpx}} = -0.68$ to -0.38).

4. DISCUSSION

$\delta^{26}\text{Mg}$ values in constituent minerals in peridotites and garnet pyroxenites or eclogites deviate considerably from the mantle average calculated from the available peridotite and oceanic basalt data ($\delta^{26}\text{Mg} = -0.245 \pm 0.119$, 2 S.D., $n = 349$; Fig. 1; supplementary data). Calculated or measured whole rock values in peridotites and garnet pyroxenites or eclogites, however, are in most cases within uncertainty of the mantle average. Inter-mineral Mg isotope variability in mantle derived rocks is thus expected to reflect temperature-dependent equilibrium isotope fractionation during magmatic processes. Especially mineral pairs with comparatively large isotopic differences, such as olivine and spinel could therefore be useful geothermometers (Young et al., 2009; Liu et al., 2011; ; Schauble, 2011; Macris et al., 2013; Xiao et al., 2013). However, compositional effects on inter-mineral isotope fractionation may affect the underlying temperature driven Mg isotope fractionation (e.g., Young et al., 2009; Liu et al., 2011; Schauble, 2011; Macris et al., 2013). Additional complexity –on the mineral or whole rock scale– may be introduced by diffusion (e.g., Huang et al., 2011; Pogge von Strandmann et al., 2011; Sio et al., 2013; Oeser et al.,

2015), metasomatic processes (Young et al., 2009; Huang et al., 2011; Xiao et al., 2013; Hu et al., 2016), and subsolidus re-equilibration of mineral phases. In light of these potential complications we will discuss the applicability of the two most promising mineral pairs for Mg isotope geothermometry: olivine–spinel (Young et al., 2009; Liu et al., 2011; Schauble, 2011; Macris et al., 2013; Xiao et al., 2013) and garnet–clinopyroxene. To minimize potential disequilibrium effects by natural or analytical processes, the following discussion will only use literature data where $\Delta^{25}\text{Mg}'$ indicates $\delta^{25}\text{Mg}$ and $\delta^{26}\text{Mg}$ within 3% of equilibrium (i.e., $-0.03 < \Delta^{25}\text{Mg}' < 0.03$; where $\Delta^{25}\text{Mg}' = \delta^{25}\text{Mg}' - 0.521 * \delta^{26}\text{Mg}'$ (Young and Galy, 2004)).

4.1. Inter-mineral Mg isotope fractionation in mantle rocks

4.1.1. Mg isotope fractionation between olivine and spinel

Theoretical and experimental studies predict up to per mill level Mg equilibrium isotope fractionation between olivine and spinel at magmatic temperatures, caused by differences in Mg–O bond length for the sixfold coordinated Mg^{2+} in olivine and mostly four-fold coordinated Mg^{2+} in spinel (Schauble, 2011; Macris et al., 2013). In spinels –with a general composition of AB_2O_4 – theory predicts that Mg–O bond length of the tetrahedral A site depends on which cation occupies the octahedral B site (Schauble, 2011). The Mg–O bond length in MgAl_2O_4 (1.964 Å) is shorter than in MgCr_2O_4 (2.001 Å) (Schauble, 2011), leading to a preference for the heavy Mg isotope in MgAl_2O_4 relative to MgCr_2O_4 . In addition to the general temperature dependence, therefore, $\Delta^{26}\text{Mg}_{\text{ol-sp}}$ should vary systematically with the relative amount of Cr in the octahedral B site, that is, the Cr# in spinel (Fig. 3). The theoretically predicted range in Mg–O bond lengths (1.964–2.001 for Cr# 0–1, (Schauble, 2011)) is on the same order as the Mg–O bond length in natural spinels (1.945–1.965 for Cr# 0–0.3; (Princivalle et al., 1989)), suggesting that theoretical predictions should also apply to natural spinels, at least qualitatively. As shown in Fig. 3a, high Cr# and high temperature for olivine–spinel equilibration predict low $\Delta^{26}\text{Mg}_{\text{ol-sp}}$.

In peridotites, the Cr# in spinel increases with the extent of melting experienced (Dick and Bullen, 1984). In absence of volatile induced, or redox partial melting, larger degrees of melting occur at higher temperatures. In this case, peridotites with increasing Cr# should reflect higher melting temperatures, and show progressively decreasing $\Delta^{26}\text{Mg}_{\text{ol-sp}}$. For peridotites with a simple petrogenetic history of melt depletion, a strong inverse coupling between $\Delta^{26}\text{Mg}_{\text{ol-sp}}$ and Cr# would thus be expected (Fig. 3a). However, few, if any of the peridotites analyzed for Mg isotope ratios preserve such a simple petrogenetic history (Fig. 4). The only likely candidate are peridotites from the North China Craton investigated by Liu et al. (2011). These rocks preserve the expected correlation between Al_2O_3 (whole rock) or Cr# in spinel with Mg# (olivine) for variably depleted residual peridotites (Fig. 4), although their rare earth element patterns also show variable metasomatic overprint (Wu et al., 2006). All other peridotite suites that include data for $\delta^{26}\text{Mg}$ in spinel have experienced considerable post-depletion metasomatism by interaction with silicate melts (Liu

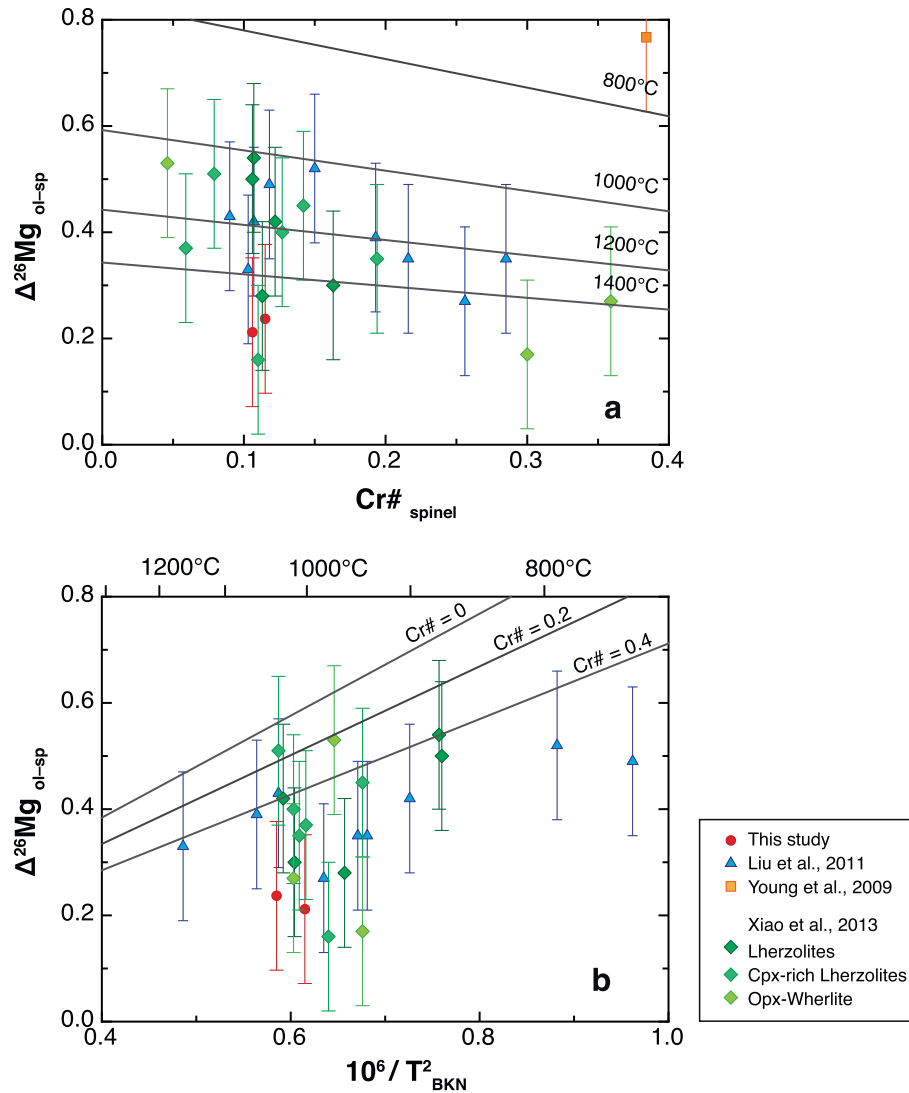


Fig. 3. (a) Diagram showing $\Delta^{26}\text{Mg}_{\text{olivine-spinel}}$ versus $\text{Cr}\#$ in spinel, and (b) $\Delta^{26}\text{Mg}_{\text{olivine-spinel}}$ versus $10^6/T_{\text{BKN}}^2$ for the peridotites with reported Mg isotope ratios in spinel. The $\text{Cr}\#$ is the molar ratio $\text{Cr}/(\text{Cr} + \text{Al})$, $\text{Mg}\#$ is the molar ratio $\text{Mg}/(\text{Mg} + \text{Fe}^{2+})$, and T_{BKN} is the Mg-Fe exchange temperature between clino- and orthopyroxene, estimated after Brey and Köhler (1990) for an assumed equilibration pressure of 15 kb, and $\Delta^{26}\text{Mg}_{\text{olivine-spinel}} = |(\delta^{26}\text{Mg}_{\text{ol}} - \delta^{26}\text{Mg}_{\text{sp}})|$. There is no systematic decrease in $\Delta^{26}\text{Mg}_{\text{olivine-spinel}}$ with $\text{Cr}\#$ in spinel, as would be expected based on theoretical predictions for refractory peridotites, nor a systematic relation between $\Delta^{26}\text{Mg}_{\text{olivine-spinel}}$ and $10^6/T_{\text{BKN}}^2$, suggesting that secondary processes (post-melting metasomatism) have disturbed these predicted primary relations. Gray lines are drawn using predictions by Schauble, (2011) and Macris et al., (2013). The $\Delta^{26}\text{Mg}_{\text{olivine-spinel}}$ for peridotites with different $\text{Cr}\#$ are linearly interpolated between the predicted $\Delta^{26}\text{Mg}_{\text{olivine-spinel}}$ for pure MgCr_2O_4 and MgAl_2O_4 (Schauble, 2011; Macris et al., 2013). Note that there is an offset between the temperatures inferred for $\Delta^{26}\text{Mg}_{\text{olivine-spinel}}$ from theoretical models (Schauble, 2011, Macris et al., 2013) and Mg-Fe exchange equilibria in pyroxenes (T_{BKN} , Brey and Köhler, 1990). Error bars for $\Delta^{26}\text{Mg}_{\text{olivine-spinel}}$ are drawn assuming an uncertainty of $\pm 0.10\%$ (2 S. D.) on $\delta^{26}\text{Mg}_{\text{ol}}$ and $\delta^{26}\text{Mg}_{\text{sp}}$, and thus a propagated uncertainty on $\Delta^{26}\text{Mg}_{\text{ol-sp}}$ of $\pm 0.14\%$ (2 S.D.) for all samples. Data and references for the major element data are given in the supplementary information.

et al., 2011; Xiao et al., 2013; Young et al., 2009), including the Hawaiian peridotites investigated in this study (Bizimis et al., 2004). Melt-peridotite reaction incongruently dissolves pyroxenes and forms olivine, spinel, and a modified melt (Kelemen et al., 1990). Melt-rock reaction, especially at lower temperature than for the primary depletion by partial melting, can therefore disturb the primary, partial melting-related $\Delta^{26}\text{Mg}_{\text{ol-sp}}$ and $\text{Cr}\#$ signatures (Fig. 3a). Hence a first-order control by temperature on $\Delta^{26}\text{Mg}_{\text{ol-sp}}$ is difficult to establish in natural peridotites investigated

for Mg isotopes thus far, because of the almost ubiquitous and variable overprint by post-melting metasomatism (e.g., Young et al., 2009; Huang et al., 2011; Xiao et al., 2013; Hu et al., 2016). Note that even for the suite of spinel peridotites from the North China Craton, the inferred temperature control on $\Delta^{26}\text{Mg}_{\text{ol-sp}}$ by Liu et al. (2011) is difficult to establish given analytical uncertainty and superimposed compositional effects due to variable $\text{Cr}\#$, which make it difficult to assign the observed variation in $\Delta^{26}\text{Mg}_{\text{ol-sp}}$ solely to temperature (Fig. 3a).

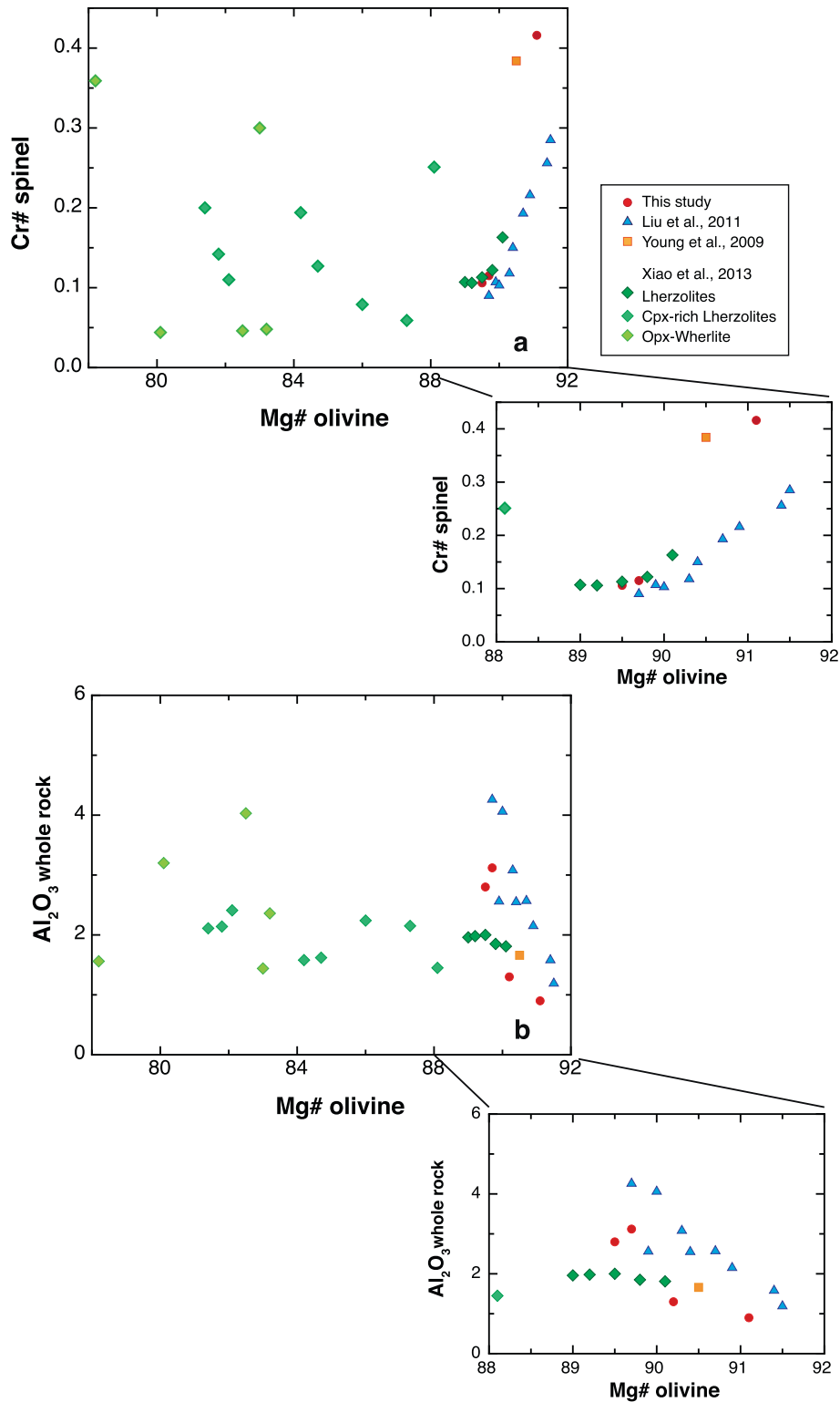


Fig. 4. Diagram showing (a) Cr# in spinel versus Mg# in olivine, and (b) Al₂O₃ (wt.%) in the whole rock versus Mg# in olivine for the peridotites with reported Mg isotope ratios in spinel. For peridotites with a simple history of depletion by partial melting, a positive correlation in (a) and a negative correlation in (b) would be expected. With the possible exception of the peridotites investigated by Liu et al. (2011), the lack of such correlations indicate that the investigated peridotite suites are affected by post-melting melt-rock reaction (metasomatism, see also Fig. 4). Further explanations are given in the main text. Data and references for the major element data are given in the supplementary information.

Moreover, a discrepancy of several hundred °C is observed between temperatures predicted from $\Delta^{26}\text{Mg}_{\text{ol-sp}}$ (Schauble, 2011) and mineral equilibria (e.g., cpx–opx, (Brey and Köhler, 1990), compare Fig. 3a and b). This discrepancy is observed for the Hawaiian peridotite xenoliths, but also for the peridotites investigated previously (Young et al., 2009; Liu et al., 2011; Xiao et al., 2013), and may point either to an offset in calculated temperatures from $\Delta^{26}\text{Mg}_{\text{ol-sp}}$, or different closure temperatures of Mg isotope exchange between olivine and spinel relative to Fe–Mg exchange between orthopyroxene and clinopyroxene (Brey and Köhler, 1990; Wells, 1977). It should also be considered that, owing to the shallow slope of the predicted $\Delta^{26}\text{Mg}_{\text{ol-sp}}$ – temperature curves (Fig. 3b; (Schauble, 2011; Macris et al., 2013)), the uncertainties in predicted temperatures from Mg isotope variations are several hundred °C at temperatures >1000 °C, assuming an uncertainty of $\pm 0.10\%$ (2 S.D.) on $\delta^{26}\text{Mg}_{\text{ol}}$ and $\delta^{26}\text{Mg}_{\text{sp}}$, and thus a propagated uncertainty on $\Delta^{26}\text{Mg}_{\text{ol-sp}}$ of $\pm 0.14\%$ (2 S.D.). For current analytical uncertainties, therefore, temperatures predicted from $\Delta^{26}\text{Mg}_{\text{ol-sp}}$ are less precise, and may also be less accurate than those derived from conventional geothermometers (e.g., (Roeder et al., 1979; Wan et al., 2008)). It should be noted, however, that different geothermometers may also diverge by over 200 °C, even in well-equilibrated peridotite and pyroxenite mantle xenoliths (Nimis and Grütter, 2010).

4.1.2. Mg isotope fractionation between garnet and clinopyroxene

Mg occupies the 8-fold coordinated A site in garnet with a general formula $\text{A}_3\text{B}_2\text{Si}_3\text{O}_{12}$. The 3+ cations Fe, Al, and Cr occupy the octahedral B site in garnet. Huang et al. (2013) inferred from theory that Mg–O bond length, and

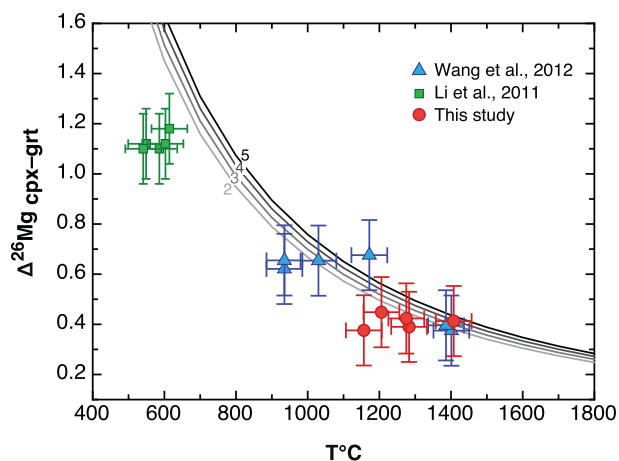


Fig. 5. Diagram showing $\Delta^{26}\text{Mg}_{\text{cpx-grt}}$ versus temperatures estimated based Fe–Mg exchange (Ellis and Green, 1979). The gray curves show the $\Delta^{26}\text{Mg}_{\text{cpx-grt}}$ – T parameterization of Huang et al. (2013) for pressures between 2 and 5 GPa. The Hawaiian pyroxenites equilibrated at a mean pressure of ~ 2.5 GPa (Bizimis et al., 2005), the pressure of equilibration for the data from Li et al. (2011) is 3 GPa and 5 GPa for the eclogites studied by Wang et al. (2012). Data from Hu et al. (2016) are omitted, because their clinopyroxene–garnet isotope ratios indicate isotopic disequilibrium.

thus Mg isotope fractionation in garnet, is largely insensitive to variable cation composition on both the A and B sites, and could thus serve as a thermobarometer (Huang et al., 2013).

For the eclogites studied by Wang et al. (2012), which are interpreted as metamorphosed altered oceanic crust, temperatures estimated from Fe–Mg exchange in clinopyroxene–garnet (Ellis and Green, 1979) and those predicted by $\Delta^{26}\text{Mg}_{\text{cpx-grt}}$ (Huang et al., 2013) agree within uncertainty (Fig. 5). The eclogites from the Dabie orogen investigated by Li et al. (2011) are ultra-high-pressure (UHP) metamorphic eclogites with gabbroic protoliths. The temperatures estimated from $\Delta^{26}\text{Mg}_{\text{cpx-grt}}$ (Huang et al., 2013) for these samples are 100–200 °C higher than the Fe–Mg exchange temperatures (549–614 °C). At these low temperatures, uncertainties in predicted temperatures are little influenced by the analytical uncertainty on $\Delta^{26}\text{Mg}_{\text{cpx-grt}}$ ($\pm 0.14\%$, see above) and are ca. ~ 50 –70 °C, (Fig. 5a). Hence the observed discrepancy likely arises from uncertainties in estimating Fe^{3+} contents from Fe_{total} in these mineral phases, which leads to anomalously low Fe–Mg exchange temperatures well outside the calibrated temperature range of this empirical thermobarometer (Ellis and Green, 1979).

The Hawaiian garnet pyroxenites analyzed in this study are interpreted as high–pressure (2–3 GPa) cumulates from melts erupted during the rejuvenated phase of volcanism (Bizimis et al., 2005; Sen et al., 2005). The temperatures of last equilibration estimated from Fe–Mg exchange (Bizimis et al., 2005) and Mg isotope fractionation for three out of five Hawaiian samples are within 40–80 °C, and therefore considered in good agreement. The other two samples show larger deviations: 140 and 260 °C, respectively. The largest difference of 260 °C is for sample 77SL-620 with a $T \sim 1160$ °C based on Fe–Mg exchange (Bizimis et al., 2005), but a $T \sim 1420$ °C based on $\Delta^{26}\text{Mg}_{\text{cpx-grt}} = 0.38$ (Table 1, Fig. 5). Although a seemingly large difference, it should be considered that uncertainties of $\pm 0.14\%$ on $\Delta^{26}\text{Mg}_{\text{cpx-grt}}$ (see above) translate into uncertainties in temperature of ~ 150 –250 °C at $T \sim 1200$ °C (Fig. 5a). Considering analytical uncertainties on $\Delta^{26}\text{Mg}_{\text{cpx-grt}}$, temperatures estimated from Fe–Mg exchange and $\Delta^{26}\text{Mg}_{\text{cpx-grt}}$ therefore mostly agree within uncertainty (Fig. 5a).

4.2. Bulk rock Mg isotope fractionation during magmatic processes

Mantle–derived rocks (i.e., peridotites, basalts) exhibit a small range in $\delta^{26}\text{Mg}$ from -0.48 to about 0 (Fig. 6; supplementary data). The global averages of peridotites ($\delta^{26}\text{Mg} = -0.243\% \pm 0.135$, 2 S.D., $n = 184$), mid ocean ridge basalts (MORB; $\delta^{26}\text{Mg} = -0.239\% \pm 0.102$, 2 S.D., $n = 74$) and ocean island basalts (OIB; $\delta^{26}\text{Mg} = -0.252\% \pm 0.096$, 2 S.D., $n = 91$) are identical within uncertainty and have similar variance (supplementary Fig. 2). Accordingly, previous studies have concluded that neither partial melting nor crystal fractionation significantly affect the Mg isotope variability of oceanic basalts on the bulk sample scale (Teng et al., 2007; Bourdon et al., 2010; Dauphas et al., 2010; Teng et al., 2010a; Huang et al., 2011). Magmatic differentiation at shallow depths (<1 GPa) in basaltic melts dominantly

involves phases whose Mg isotope composition is similar to that of the bulk rock (olivine, Fig. 1), or phases that contain little Mg (plagioclase). Thus, fractional crystallization of basaltic melts does not produce significant Mg isotope fractionation (e.g., Teng et al., 2007), unless large amounts of clinopyroxene with slightly different Mg isotope composition compared to the bulk rocks (Fig. 1) dominate the fractionating assemblage. Partial melting in Earth's mantle, however, preferentially consumes clinopyroxene and garnet, which have $\delta^{26}\text{Mg}$ significantly different from the average bulk mantle (Fig. 1), and may therefore induce isotopic differences between melt (basalt) and residue (peridotite) (Zhong et al., 2017). If so, this needs to be reconciled with the identical average $\delta^{26}\text{Mg}$ of basalts and peridotites.

In the following, Mg isotope fractionation during partial melting of mantle lithologies is investigated using an incremental non-modal melting model, equivalent to fractional melting (Shaw, 1970). For details of the modeling see the [supplementary information](#). In the absence of experimentally determined mineral–melt isotope fractionation factors, $\alpha_{\text{mineral-melt}}$, these can be estimated from known inter-mineral isotope fractionation factors (Fig. 2), and one known or estimated $\alpha_{\text{mineral-melt}}$ (cf. Williams and Bizimis, 2014; Zhong et al., 2017) as a reference point. Olivine and orthopyroxene are isotopically almost identical to bulk peridotite and basaltic melts, and thus have $\alpha_{\text{ol,opx-melt}} \sim 1$ (Figs. 1, 2, and [supplementary Fig. 2](#)). Moreover, Mg occurs in five to six-fold coordination in silicate melts (George and Stebbins, 1998; Shimoda et al., 2007), similar to Mg in olivine and orthopyroxene, providing additional support for the assumption that little, if any, isotope fractionation between olivine or orthopyroxene and melt occurs. Alternatively, minimum $\alpha_{\text{mineral-melt}}$ can be calculated from known inter-mineral isotope fractionation factors (Fig. 2) and assuming an initial

$\alpha_{\text{source-melt}} = 1$, which appears reasonable for Mg, because peridotites and basalts have, on average, almost identical $\delta^{26}\text{Mg}$ (Fig. 1, [supplementary Fig. 2](#)). The latter approach anchors the initial melt at the initial $^{26}\text{Mg}/^{24}\text{Mg}$ of the residue (initial $\alpha_{\text{source-melt}} = 1$, Fig. 7), but would offset the initial $^{26}\text{Mg}/^{24}\text{Mg}$ of the melt from its source for $\alpha_{\text{source-melt}} \neq 1$. The former approach for calculating initial $\alpha_{\text{source-melt}}$ offsets the initial $^{26}\text{Mg}/^{24}\text{Mg}$ of the melt to that of the peridotite source proportional to the difference between the $^{26}\text{Mg}/^{24}\text{Mg}$ of olivine (orthopyroxene) and the bulk peridotite. For melting garnet pyroxenite sources, $\alpha_{\text{cpx,grt-melt}}$ can also be calculated from known inter-mineral isotope fractionation factors (Fig. 2) and assuming $\alpha_{\text{source-melt}} = 1$, or, $\alpha_{\text{cpx,grt-melt}}$ similar to those derived for peridotite–melt can be used. Similar to the peridotite case, the initial melt is either anchored or slightly offset from the initial $^{26}\text{Mg}/^{24}\text{Mg}$ of the garnet pyroxenite. It should be stressed that the inherent assumptions for calculating $\alpha_{\text{source-melt}}$ are critical for assessing the overall isotopic offset between source and melt (cf. Williams and Bizimis, 2014; Zhong et al., 2017). Importantly, the magnitude of isotope fractionation between source and melt remains uncertain in the absence of experimentally determined $\alpha_{\text{mineral-melt}}$, but the relative changes in $^{26}\text{Mg}/^{24}\text{Mg}$ ($\delta^{26}\text{Mg}$) of melt and residue with progressive melting are independent of their initial values and are thus a robust feature for any given melting scenario. The following discussion of the effect of partial melting on the $\delta^{26}\text{Mg}$ of the derivative melts will therefore focus on these relative changes in $\delta^{26}\text{Mg}$ with progressive melting. In Fig. 6, all $\alpha_{\text{mineral-melt}}$ are estimated assuming the initial $\alpha_{\text{source-melt}} = 1$, hence are initially anchored at their source value, but it should be kept in mind that larger offsets between melt and residue would occur for initial $\alpha_{\text{source-melt}} \neq 1$.

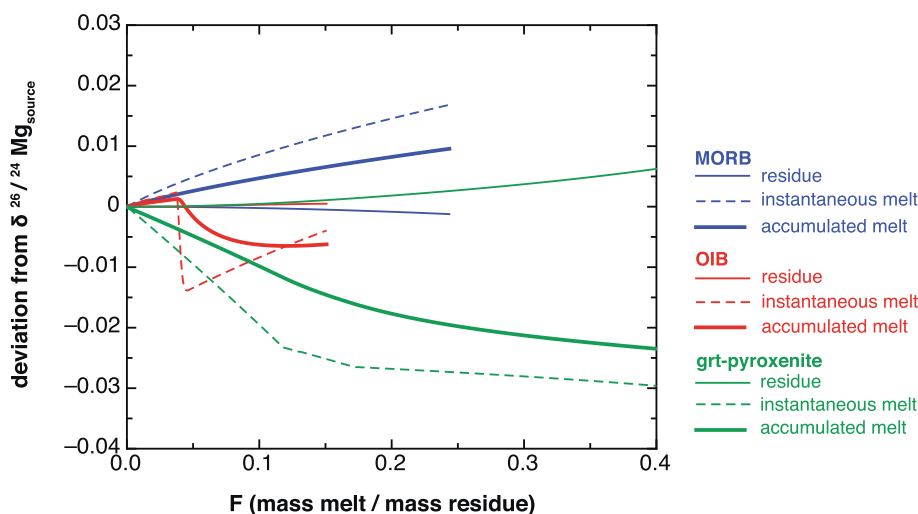


Fig. 6. Diagram showing the deviation in $\delta^{26}\text{Mg}$ of instantaneous and accumulated melts and residue from the initial source composition for melting spinel peridotite (MORB), garnet peridotite (OIB), and garnet pyroxenite. F is the extent of melting, i.e., the mass of melt generated relative to the mass of the source. The $\delta^{26}\text{Mg}$ of the partial melts become different from their source value owing to the changing contribution of Mg from the different source minerals to the melt. Garnet has a large influence on the $\delta^{26}\text{Mg}$ of the partial melt, but the calculated variation in $\delta^{26}\text{Mg}$ is small ($\sim 0.03\%$) relative to the typical analytical uncertainty of $\sim 0.1\%$. Note that $\alpha_{\text{mineral-melt}}$ used in the calculations are calculated from known inter-mineral isotope fractionation factors (Fig. 2) and assuming an initial $\alpha_{\text{source-melt}} = 1$, hence the calculated deviations from the initial source are minimum deviations, and the overall offset to the initial source could be larger for any initial $\alpha_{\text{source-melt}} \neq 1$. Further details of the partial melting calculations are described in the text and the [supplementary information](#).

Fig. 6 shows that for melting garnet peridotite at high P-T (OIB melting), melts evolve to slightly lower $\delta^{26}\text{Mg}$ compared to their initial value, but only by $<0.01\%$. The changing $\delta^{26}\text{Mg}$ of the partial melts with increasing extent of melting (F) reflect the changing contribution of Mg of each mineral to the melt. For the melt reactions assumed here, formation of orthopyroxene, and consumption of clinopyroxene and garnet characterize the melting of garnet peridotite at high P and low F. During this early stage of melting, clinopyroxene delivers approximately four times more Mg to the melts than garnet, thus outweighs the effect of melting garnet with $\delta^{26}\text{Mg}$ lower than the bulk peridotite. During the rapid transition from garnet to spinel peridotite, spinel (and orthopyroxene) is formed at the expense of garnet (and olivine) and a large amount of Mg from garnet enters the melt, thus decreasing its $\delta^{26}\text{Mg}$. Eventually, after garnet disappears from the residue, almost only clinopyroxene delivers Mg to the produced melt, which slightly increases the $\delta^{26}\text{Mg}$ in the incremental melts. During melting of peridotite at comparatively lower P-T (MORB melting), garnet is residual only during the initial stages, or absent from the residual assemblage. In this latter case, melting is dominated by clinopyroxene, and the $\delta^{26}\text{Mg}$ of the produced melts increase in $\delta^{26}\text{Mg}$, but still remains within $<0.01\%$ of its starting value (Fig. 6). Overall, partial melting of peridotite therefore does not produce resolvable Mg isotope variation, unless the assumption inherent in calculating $\alpha_{\text{source-melt}}$ lead to values substantially different from 1 (cf. Zhong et al., 2017). The reason is that the $\alpha_{\text{source-melt}}$ is buffered ~ 1 by residual olivine and orthopyroxene, which together host ca. 90% of the Mg and have $\alpha_{\text{ol,opx-melt}} \sim 1$ (Fig. 1).

More significant Mg isotope fractionation during partial melting is expected only if the predominant contribution of Mg is from phases with $\delta^{26}\text{Mg}$ significantly different from that of the bulk rock. Melting of mafic lithologies, such as garnet pyroxenite, imposes a pronounced garnet signature onto the derivative melts, and thus results in $\delta^{26}\text{Mg}$ variability in excess of that for peridotite melting (Fig. 6). Melts of G2 pyroxenite are dominated by melting garnet at low extent of melting, but are increasingly dominated by melting clinopyroxene with progressive extent of melting (Pertermann and Hirschmann, 2003a, b). Owing to the persistent strong garnet influence, the $\delta^{26}\text{Mg}$ of garnet pyroxenite melts remains lower than their starting value, by ca. 0.03–0.04‰, even for extents of melting $>50\%$ (Fig. 6). However, the $\delta^{26}\text{Mg}$ of garnet pyroxenite melts strongly depend on the relative contribution of Mg from clinopyroxene and garnet. Below ca. 12% of melting, garnet delivers more Mg to the melt than clinopyroxene, which is reversed at $F > 12\%$ (Fig. 6), and garnet pyroxenite melts then deviate less from that of the bulk residue, similar to what is observed for peridotite-derived melts.

In the OIB investigated thus far, the lowest $\delta^{26}\text{Mg}$ in OIB occur in rocks with the highest Sm/Yb and tend to decrease with increasing Sm/Yb (Fig. 7). This observation is consistent with the greater influence of residual garnet during melting predicted by our model. Some scatter is induced by variable amounts of clinopyroxene accumulation or fractionation (Fig. 7), but the available data hint at a possible decrease of $\delta^{26}\text{Mg}$ with progressively lower degrees of melting in the garnet–stability field, that is, higher Sm/Yb (Fig. 7). As discussed above, $\delta^{26}\text{Mg}$ significantly lower than their initial source are only expected for

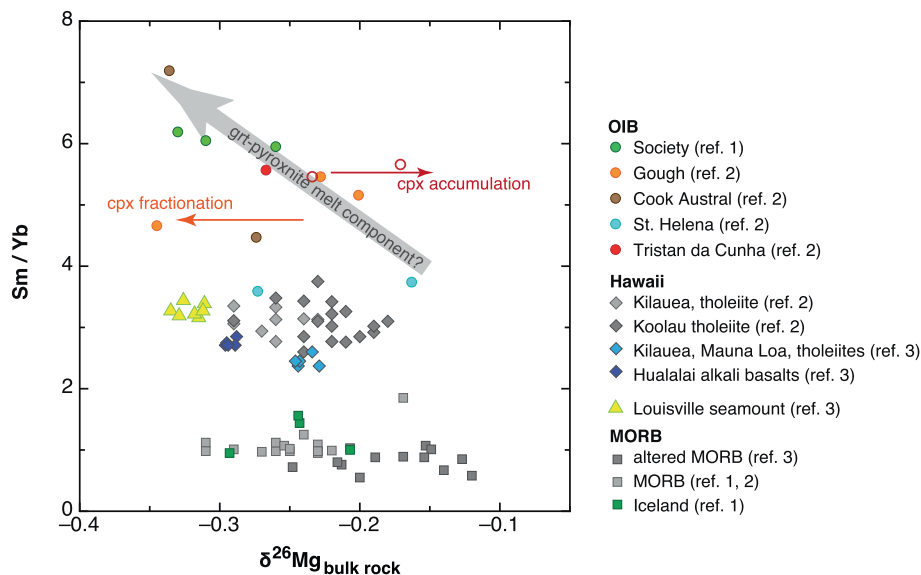


Fig. 7. Observed variation between bulk rock $\delta^{26}\text{Mg}$ and Sm/Yb in OIB and MORB. Data are grouped in (1) OIB from the South Pacific and South Atlantic, which are created by small amounts of melting in the garnet stability field (colored circles), (2) OIB created by large amounts of melting in the garnet stability field with intermediate Sm/Yb (Hawaii, diamonds), and (3) ridge basalts (squares) including those from Iceland (green squares), which are dominated by melting in the spinel stability field with Sm/Yb ~ 1 (Fig. 7c). The Mg isotope data are taken from Ref. 1: Bourdon et al. (2010), Ref. 2: Teng et al. (2010a), and Ref. 3: Zhong et al. (2017). Data and references for the trace element data are given in the supplementary information. (For interpretation of the references to color in this figure legend, the reader is referred to the web version of this article.)

melting garnet pyroxenite, and this observation could therefore be indicative of an increasing garnet pyroxenite melt component in OIB with increasingly lower $\delta^{26}\text{Mg}$. Confidently resolving this effect, however, would require larger absolute values of $\alpha_{\text{mineral-melt}}$ than the minimum values assumed for the modeling in this study, or, alternatively more precise Mg isotope data (see discussion above and Fig. 7). Whereas the data for Hawaiian alkali basalts compared to tholeiites by Zhong et al. (2017) are compatible with such an interpretation, the data for Hawaiian tholeiites reported previously (Teng et al., 2010a) do not show any systematic variation in Fig. 7. Although this observation is consistent with the small variability of Sm/Yb and $\delta^{26}\text{Mg}$ at the similarly large degrees of melting expected for Hawaiian tholeiites, significant analytical uncertainty in the $\delta^{26}\text{Mg}$ and the trace element data compiled for the Hawaiian tholeiites (see Fig. 7 and supplementary data) – but also variable amounts of clinopyroxene fractionation – may obscure an inherent systematic relationship as observed by Zhong et al. (2017). In MORB (including Iceland) the invariably low Sm/Yb reflect large amounts of melting in the spinel–stability field (Figs. 6 and 7). $\delta^{26}\text{Mg}$ in MORB scatter around the MORB average ($-0.239\text{‰} \pm 0.102$, S.D., $n = 74$; supplementary data), probably mostly due to analytical uncertainty in $\delta^{26}\text{Mg}$, but some low $\delta^{26}\text{Mg}$ could also be consistent with a garnet pyroxenite melt component. It should also be noted that the relatively large extents of melting for MORB and the Hawaiian tholeiites make it difficult to resolve potential pyroxenite $\delta^{26}\text{Mg}$ signatures. For melting of lithologically heterogeneous mantle sources, the relative contribution of pyroxenite–derived melt to the erupted melt decreases with increasing extent of (peridotite) melting (c.f. Stracke and Bourdon, 2009). Large overall extents of partial melting also minimize any variation in Sm/Yb, thus making it more difficult to resolve correlated small differences in $\delta^{26}\text{Mg}$ in pyroxenite versus peridotite–derived melts, especially in light of the current analytical uncertainty on $\delta^{26}\text{Mg}$.

4.3. Applications for Mg isotope fractionation during magmatic processes

Several studies highlighted the potential application of large inter–mineral olivine–spinel fractionation as a geothermometer in peridotites (Young et al., 2009; Liu et al., 2011; Schauble, 2011; Xiao et al., 2013). A dominant effect of temperature on $\Delta^{26}\text{Mg}_{\text{ol-sp}}$, however, can only be expected for refractory peridotites with a simple petrogenetic history by melt depletion. In this case a superimposed compositional effect on Mg isotope fractionation in spinel, that is, decreasing $\Delta^{26}\text{Mg}_{\text{ol-sp}}$ with increasing Cr# in spinel (Fig. 3, (Schauble, 2011)), should further diminish the decreasing $\Delta^{26}\text{Mg}_{\text{ol-sp}}$ with increasing temperature. However, most of the peridotites analyzed for Mg isotopes so far do not preserve such a simple petrogenetic history, but have $\Delta^{26}\text{Mg}_{\text{ol-sp}}$ that are variably overprinted by metasomatism (melt–rock reaction, Fig. 4). A possible exception may be the peridotites from the North China Craton investigated by Liu et al. (2011). Even in this latter case, however, disentangling temperature and compositionally

related effects on $\Delta^{26}\text{Mg}_{\text{ol-sp}}$ proves complicated (Fig. 3a), making olivine–spinel Mg isotope fractionation in peridotites a difficult–to–apply geothermometer. Moreover, in addition to melt–rock reaction (metasomatism) subsolidus re-equilibration, diffusion (e.g., Huang et al., 2011; Pogge von Strandmann et al., 2011; Sio et al., 2013; Oeser et al., 2015), or surface alteration may also affect the Mg isotope composition of olivine and spinel in mantle peridotites.

In contrast to olivine–spinel, inter–mineral Mg isotope fractionation between co–existing clinopyroxene and garnet (Li et al., 2011; Wang et al., 2012; Wang et al., 2014; and this study) is a more promising geothermometer (see also Huang et al., 2013). However, significant deviations between temperatures estimated from Mg isotope fractionation and Fe–Mg exchange between cpx and grt are observed, mostly at $T < 800\text{ °C}$, probably due to anomalously low Fe–Mg exchange temperatures resulting from uncertainties in estimating Fe^{3+} – Fe^{2+} contents (Ellis and Green, 1979). Uncertainties on temperature estimates from $\Delta^{26}\text{Mg}_{\text{cpx-grt}}$ at higher magmatic temperatures may arise mostly from analytical uncertainty in $\Delta^{26}\text{Mg}_{\text{cpx-grt}}$ ($\sim \pm 0.14\text{‰}$) which is several 100 °C at $T > 1100$ – 1200 °C (Huang et al., 2013), Fig. 5). Precise temperature estimates based on $\Delta^{26}\text{Mg}_{\text{cpx-grt}}$ are thus only possible within a small temperature range between $T \sim 800$ – 1100 °C , restricting its use to garnet–bearing igneous and metamorphic rocks. It should also be assessed whether the potential information to be derived from Mg isotope thermobarometry warrants the substantially larger analytic effort compared to conventional Fe–Mg exchange thermobarometers.

Applications of Mg isotope fractionation on the bulk sample scale in magmatic rocks have so far been elusive, because of the associated small range of $\delta^{26}\text{Mg}$. Zhong et al. (2017) recently argued that partial melting leads to Mg isotope fractionation on a level of tenths of per mill. However, the observation that olivine and orthopyroxene have similar $\delta^{26}\text{Mg}$ as both average peridotite and basalts (Figs. 1, 2, and supplementary Fig. 2) indicates that $\alpha_{\text{ol, opx-melt}} \sim 1$. Given the predominance of olivine and orthopyroxene on the Mg budget of peridotite, partial melting of peridotite does not result in resolvable Mg isotope fractionation, in good agreement with the identical average $\delta^{26}\text{Mg}$ in peridotites and basalts (supplementary Fig. 2). More variable $\delta^{26}\text{Mg}$ may only result from melting mafic source lithologies such as garnet pyroxenite, consistent with a tendency of lower $\delta^{26}\text{Mg}$ with higher Sm/Yb (Fig. 7). At current levels of analytical precision, however, this effect is only resolvable with confidence for larger absolute values of $\alpha_{\text{mineral-melt}}$ than assumed for the modeling in this study (Fig. 6). Low $\delta^{26}\text{Mg}$ at high Sm/Yb observed in some alkaline OIB, however, hint at a possible signature of garnet pyroxenite melting, in which case $\delta^{26}\text{Mg}$ trace lithological mantle heterogeneity. In contrast, the higher extents of melting inferred for tholeiitic OIB and especially MORB, lead to much less variable Sm/Yb than in the low degree alkaline OIB, making it difficult to resolve potentially correlated sub per mill variations in $\delta^{26}\text{Mg}$.

Owing to the general lack of offset in $\delta^{26}\text{Mg}$ between mantle sources and melt (supplementary Fig. 2), Mg isotope ratios in mantle–derived rocks should accurately reflect bulk

planetary composition. Hence, comparison of $\delta^{26}\text{Mg}$ in meteorites and bulk planets could provide valuable information about the provenance of planet forming materials, and the processes that lead to Mg isotope fractionation during planet formation and early differentiation. However, while some earlier studies invoke a difference between silicate Earth and chondrites (Wiechert and Halliday, 2007; Young et al., 2009), most recent studies have argued for a broadly similar Mg isotope composition (Yang et al., 2009; Handler et al., 2009; Bourdon et al., 2010; Schiller et al., 2010; Teng et al., 2010a; Bizzarro et al., 2011; Huang et al., 2011; Liu et al., 2011). A compilation of the available data yields average $\delta^{26}\text{Mg}$ of -0.270% (± 0.074 , S.D., $n = 102$) in chondrites and $\delta^{26}\text{Mg} = -0.247\%$ (± 0.064 , S.D., $n = 389$) in terrestrial mantle-derived rocks (basalts, eclogites, and peridotites) (supplementary data). As pointed out by Pogge von Strandmann et al. (2011), these averages are statistically different based on a student's t-test. Recent, more precise Mg isotope measurements have substantiated this small difference in $\delta^{26}\text{Mg}$ between chondritic meteorites and the bulk silicate Earth and attributed it to vapor loss from growing planetesimals (Hin et al., 2017).

In summary, in addition to being potential geothermometers (especially clinopyroxene–garnet), stable Mg isotope variations in magmatic rocks may be a useful tool for identifying lithological heterogeneity in the mantle. Analysis of peridotitic garnets and the investigation of specifically targeted OIB suites should allow further constraints on the potential variation in $\delta^{26}\text{Mg}$ in response to partial melting. Most crucial in this respect, however, is to determine isotope fractionation factors between mantle minerals and melt, $\alpha_{\text{mineral-melt}}$, which would determine the actual offsets in $\delta^{26}\text{Mg}$ between melt and source, and thus further constrain the respective influence of different source lithologies on the $\delta^{26}\text{Mg}$ of mantle melts. Applications for high-temperature Mg isotope fractionation are thus diverse, but further improving the analytical precision of Mg isotope measurements (e.g., Hin et al., 2017) has proven crucial for planetary scale applications, and also holds promise for investigating a diverse range of magmatic processes at higher resolution.

ACKNOWLEDGMENTS

We would like to thank the reviewers, Jasper Konter, Merlin Méheut, and the associate editor Nicolas Dauphas for their helpful and constructive comments, which significantly improved parts of the discussion. Marc Norman is thanked for editorial handling. ETT was supported by a Marie-Curie Inter-European-Fellowship No. 41189 at ETH Zürich for research on global budgets of Ca and Mg and a Cambridge NERC Fellowship (NE/G013764/1) at the University of Cambridge. MB acknowledges NSF grants OCE-0622827 and OCE – 0852488 for sample collection and processing.

APPENDIX A. SUPPLEMENTARY MATERIAL

Supplementary data associated with this article can be found, in the online version, at <https://doi.org/10.1016/j.gca.2018.02.002>.

REFERENCES

- Bizimis M., Griselein M., Lassiter J. C., Salters V. J. M. and Sen G. (2007) Ancient recycled mantle lithosphere in the Hawaiian plume: osmium-hafnium isotope evidence from peridotite mantle xenoliths. *Earth Planet. Sci. Lett.* **257**, 259–273.
- Bizimis M., Salters V. J. M., Garcia M. O. and Norman M. D. (2013) The composition and distribution of the rejuvenated component across the Hawaiian plume: Hf-Nd-Sr-Pb isotope systematics of Kaula lavas and pyroxenite xenoliths. *Geochim. Geophys. Geosys.* **14**. <https://doi.org/10.1002/ggge.20250>.
- Bizimis M., Sen G. and Salters V. J. M. (2004) Hf-Nd isotope decoupling in the oceanic lithosphere. Constraints from spinel peridotites from Oahu, Hawaii. *Earth Planet. Sci. Lett.* **217**, 43–58.
- Bizimis M., Sen G., Salters V. J. M. and Keshav S. (2005) Hf-Nd-Sr isotope systematics of garnet pyroxenites from Salt Lake Crater, Oahu, Hawaii: evidence for a depleted component in Hawaiian volcanism. *Geochim. Cosmochim. Acta* **69**, 2629–2646.
- Bizzarro M., Paton C., Larsen K., Schiller M., Trinquier A. and Ulfbeck D. (2011) High-precision Mg-isotope measurements of terrestrial and extraterrestrial material by HR-MC-ICPMS-implications for the relative and absolute Mg-isotope composition of the bulk silicate Earth. *J. Analytical Atomic Spectrom.* **26**, 565–577.
- Bourdon B., Tipper E. T., Fitoussi C. and Stracke A. (2010) Chondritic Mg isotope composition of the Earth. *Geochim. Cosmochim. Acta* **74**, 5069–5083.
- Brenot A., Cloquet C., Vigier N., Carignan J. and France-Lanord C. (2008) Magnesium isotope systematics of the lithologically varied Moselle river basin, France. *Geochim. Cosmochim. Acta* **72**, 5070–5089.
- Brey G. P. and Köhler T. (1990) Geothermobarometry in four-phase lherzolites II. New thermobarometers, and practical assessment of existing thermobarometers. *J. Petrol.* **31**, 1353–1378.
- Clague D. A. and Frey F. A. (1982) Petrology and trace element chemistry of the Honolulu volcanics, Oahu: implication for the oceanic mantle below Hawaii. *J. Petrol.* **23**, 447–504.
- Dauphas N., Teng F.-Z. and Arndt N. T. (2010) Magnesium and iron isotopes in 2.7 Ga Alexo komatiites: mantle signatures, no evidence for Soret diffusion, and identification of diffusive transport in zoned olivine. *Geochim. Cosmochim. Acta* **74**, 3274–3291.
- Dick H. J. B. and Bullen T. (1984) Chromian spinel as a petrogenetic indicator in abyssal and alpine-type peridotites and spatially associated lavas. *Contrib. Mineral. Petrol.* **86**, 54–76.
- Ellis D. J. and Green D. H. (1979) An experimental study of the effect of Ca upon garnet-clinopyroxene Fe-Mg exchange equilibria. *Contrib. Mineral. Petrol.* **71**, 13–22.
- Galy A., Bar-Matthews M., Halicz L. and O'Nions R. K. (2002) Mg isotopic composition of carbonate: insight from speleothem formation. *Earth Planet. Sci. Lett.* **201**, 105–115.
- Garcia M. O., Swinnard L., Weis D., Greene A. R., Tagami T., Sano H. and Gandy C. E. (2010) Petrology, geochemistry and geochronology of Kaua'i Lavas over 4–5 Myr: implications for the origin of rejuvenated volcanism and the evolution of the Hawaiian plume. *J. Petrol.* **51**, 1507–1540.
- George A. M. and Stebbins J. F. (1998) Structure and dynamics of magnesium in silicate melts; a high-temperature 25 Mg NMR study. *Am. Mineral.* **83**, 1022–1029.
- Handler M. R., Baker J. A., Schiller M., Bennett V. C. and Yaxley G. M. (2009) Magnesium stable isotope composition of Earth's upper mantle. *Earth Planet. Sci. Lett.* **282**, 306–313.

- Hin R. C., Coath C. D., Carter P. J., Nimmo F., Lai Y.-J., Pogge von Strandmann P. A. E., Willbold M., Leinhardt Z. M., Walter M. J. and Elliott T. (2017) Magnesium isotope evidence that accretional vapour loss shapes planetary compositions. *Nature* **549**, 511–515.
- Hippler D., Buhl D., Witbaard R., Richter D. K. and Immenhauser A. (2009) Towards a better understanding of magnesium-isotope ratios from marine skeletal carbonates. *Geochim. Cosmochim. Acta* **73**, 6134–6146.
- Hu Y., Teng F.-Z., Zhang H.-F., Xiao Y. and Su B.-X. (2016) Metasomatism-induced mantle magnesium isotopic heterogeneity: evidence from pyroxenites. *Geochim. Cosmochim. Acta* **185**, 88–111.
- Huang F., Chen L., Wu Z. and Wang W. (2013) First-principles calculations of equilibrium Mg isotope fractionations between garnet, clinopyroxene, orthopyroxene, and olivine Implications for Mg isotope thermometry. *Earth Planet. Sci. Lett.* **367**, 61–70.
- Huang F., Zhang Z., Lundstrom C. C. and Zhi X. (2011) Iron and magnesium isotopic compositions of peridotite xenoliths from Eastern China. *Geochim. Cosmochim. Acta* **75**, 3318–3334.
- Kelemen P. B., Johnson K. T. M., Kinzler R. J. and Irving A. J. (1990) High-field strength element depletions in arc basalts due to mantle-magma interaction. *Nature* **345**, 521–524.
- Keshav S. and Sen G. (2001) Majoritic garnets in Hawaiian Xenoliths: preliminary results. *Geophys. Res. Lett.* **28**, 3509–3512.
- Keshav S., Sen G. and Presnall D. C. (2007) Garnet-bearing xenoliths from Salt Lake Crater, Oahu, Hawaii: high-pressure fractional crystallization in the oceanic mantle. *J. Petrol.* **48**, 1681–1724.
- Li W.-Y., Teng F.-Z., Xiao Y. and Huang J. (2011) High-temperature inter-mineral magnesium isotope fractionation in eclogite from the Dabie orogen, China. *Earth Planet. Sci. Lett.* **304**, 224–230.
- Liu S.-A., Teng F.-Z., Yang W. and Wu F.-Y. (2011) High-temperature inter-mineral magnesium isotope fractionation in mantle xenoliths from the North China craton. *Earth Planet. Sci. Lett.* **308**, 131–140.
- Macris C. A., Young E. D. and Manning C. E. (2013) Experimental determination of equilibrium magnesium isotope fractionation between spinel, forsterite, and magnesite from 600 to 800 °C. *Geochim. Cosmochim. Acta* **118**, 18–32.
- Norman M. D., Yaxley G. M., Bennett V. C. and Brandon A. D. (2006) Magnesium isotopic composition of olivine from the Earth, Mars, Moon, and pallasite parent body. *Geophys. Res. Lett.* **33**.
- Oeser M., Dohmen R., Horn I., Schuth S. and Weyer S. (2015) Processes and time scales of magmatic evolution as revealed by Fe–Mg chemical and isotopic zoning in natural olivines. *Geochim. Cosmochim. Acta* **154**, 130–150.
- Nimis P. and Grütter H. (2010) Internally consistent geothermometers for garnet peridotites and pyroxenites. *Contrib. Mineral. Petrol.* **159**, 411–427.
- Pertermann M. and Hirschmann M. M. (2003a) Anhydrous partial melting experiments on a MORB-like eclogite: phase relations phase compositions and mineral-melt partitioning of major elements at 2–3 GPa. *J. Petrol.* **44**, 2173–2201.
- Pertermann M. and Hirschmann M. M. (2003b) Partial melting experiments on a MORB-like pyroxenite between 2 and 3GPa: constraints on the presence of pyroxenite in basalt source regions from solidus location and melting rate. *J. Geophys. Res.* **108**, 215, 210.1029/2000JB000118.
- Pogge von Strandmann P. A. E., Burton K. W., James R. H., van Calsteren P., Gislason S. R. and Sigfússon B. (2008a) The influence of weathering processes on riverine magnesium isotopes in a basaltic terrain. *Earth Planet. Sci. Lett.* **276**, 187–197.
- Pogge von Strandmann P. A. E., Elliott T., Marschall H. R., Coath C., Lai Y.-J., Jeffcoate A. B. and Ionov D. A. (2011) Variations of Li and Mg isotope ratios in bulk chondrites and mantle xenoliths. *Geochim. Cosmochim. Acta* **75**, 5247–5268.
- Pogge von Strandmann P. A. E., James R. H., van Calsteren P., Gislason S. R. and Burton K. W. (2008b) Lithium, magnesium and uranium isotope behaviour in the estuarine environment of basaltic islands. *Earth Planet. Sci. Lett.* **274**, 462–471.
- Princivalle F., Della Giusta A. and Carbonin S. (1989) Comparative crystal chemistry of spinels from some suites of ultramafic rocks. *Mineral. Petrol.* **40**, 117–126.
- Roeder P., Campbell I. and Jamieson H. (1979) A re-evaluation of the olivine-spinel geothermometer. *Contrib. Mineral. Petrol.* **68**, 325–334.
- Schauble E. A. (2011) First-principles estimates of equilibrium magnesium isotope fractionation in silicate, oxide, carbonate and hexaaquamagnesium(2+) crystals. *Geochim. Cosmochim. Acta* **75**, 844–869.
- Schiller M., Handler M. R. and Baker J. A. (2010) High-precision Mg isotopic systematics of bulk chondrites. *Earth Planet. Sci. Lett.* **297**, 165–173.
- Sedaghatpour F., Teng F.-Z., Liu Y., Sears D. W. G. and Taylor L. A. (2013) Magnesium isotopic composition of the Moon. *Geochim. Cosmochim. Acta* **120**, 1–6.
- Sen G., Keshav S. and Bizimis M. (2005) Hawaiian mantle xenoliths and magmas: Composition and thermal character of the lithosphere. *Am. Mineral.* **90**, 871–887.
- Sen I. S., Bizimis M. and Sen G. (2010) Geochemistry of sulfides in Hawaiian garnet pyroxenite xenoliths: implications for highly siderophile elements in the oceanic mantle. *Chem. Geol.* **273**, 180–192.
- Sen I. S., Bizimis M., Sen G. and Huang S. (2011) A radiogenic Os component in the oceanic lithosphere? Constraints from Hawaiian pyroxenite xenoliths. *Geochim. Cosmochim. Acta* **75**, 4899–4916.
- Shaw D. M. (1970) Trace element fractionation during anatexis. *Geochim. Cosmochim. Acta* **34**, 237–243.
- Shen B., Jacobsen B., Lee C.-T. A., Yin Q.-Z. and Morton D. M. (2009) The Mg isotopic systematics of granitoids in continental arcs and implications for the role of chemical weathering in crust formation. *Proc. Natl. Acad. Sci.* **106**, 20652–20657.
- Shimoda K., Tobu Y., Hatakeyama M., Nemoto T. and Saito K. (2007) Structural investigation of Mg local environments in silicate glasses by ultra-high field 25Mg 3QMAS NMR spectroscopy. *Am. Mineral.* **92**, 695–698.
- Sio C. K. I., Dauphas N., Teng F.-Z., Chaussidon M., Helz R. T. and Roskosz M. (2013) Discerning crystal growth from diffusion profiles in zoned olivine by in situ Mg–Fe isotopic analyses. *Geochim. Cosmochim. Acta* **123**, 302–321.
- Stracke A. and Bourdon B. (2009) The importance of melt extraction for tracing mantle heterogeneity. *Geochim. Cosmochim. Acta* **73**, 218–238.
- Teng F.-Z., Dauphas N., Huang S. and Marty B. (2013) Iron isotopic systematics of oceanic basalts. *Geochim. Cosmochim. Acta* **107**, 12–26.
- Teng F.-Z., Li W.-Y., Ke S., Marty B., Dauphas N., Huang S., Wu F.-Y. and Pourmand A. (2010a) Magnesium isotopic composition of the Earth and chondrites. *Geochim. Cosmochim. Acta* **74**, 4150–4166.
- Teng F.-Z., Li W.-Y., Rudnick R. L. and Gardner L. R. (2010b) Contrasting lithium and magnesium isotope fractionation during continental weathering. *Earth Planet. Sci. Lett.* **300**, 63–71.

- Teng F.-Z., Wadhwa M. and Helz R. T. (2007) Investigation of magnesium isotope fractionation during basalt differentiation: implications for a chondritic composition of the terrestrial mantle. *Earth Planet. Sci. Lett.* **261**, 84–92.
- Tipper E. T., Bickle M. J., Galy A., West A. J., Pomiès C. and Chapman H. J. (2006a) The short term climatic sensitivity of carbonate and silicate weathering fluxes: insight from seasonal variations in river chemistry. *Geochim. Cosmochim. Acta* **70**, 2737–2754.
- Tipper E. T., Galy A. and Bickle M. J. (2006b) Riverine evidence for a fractionated reservoir of Ca and Mg on the continents: implications for the oceanic Ca cycle. *Earth Planet. Sci. Lett.* **247**, 267–279.
- Tipper E. T., Galy A. and Bickle M. J. (2008a) Calcium and magnesium isotope systematics in rivers draining the Himalaya-Tibetan-Plateau region: lithological or fractionation control? *Geochim. Cosmochim. Acta* **72**, 1057–1075.
- Tipper E. T., Galy A., Gaillardet J., Bickle M. J., Elderfield H. and Carder E. A. (2006c) The magnesium isotope budget of the modern ocean: constraints from riverine magnesium isotope ratios. *Earth Planet. Sci. Lett.* **250**, 241–253.
- Tipper E. T., Louvat P., Capmas F., Galy A. and Gaillardet J. (2008b) Accuracy of stable Mg and Ca isotope data obtained by MC-ICP-MS using the standard addition method. *Chem. Geol.* **257**, 65–75.
- Wan Z., Coogan L. A. and Canil D. (2008) Experimental calibration of aluminum partitioning between olivine and spinel as a geothermometer. *Am. Mineral.* **93**, 1142–1147.
- Wang S.-J., Teng F.-Z., Li S.-G. and Hong J.-A. (2014) Magnesium isotopic systematics of mafic rocks during continental subduction. *Geochim. Cosmochim. Acta* **143**, 34–48.
- Wang S.-J., Teng F.-Z. and Scott J. M. (2016) Tracing the origin of continental HIMU-like intraplate volcanism using magnesium isotope systematics. *Geochim. Cosmochim. Acta* **185**, 78–87.
- Wang S.-J., Teng F.-Z., Williams H. M. and Li S.-G. (2012) Magnesium isotopic variations in cratonic eclogites: origins and implications. *Earth Planet. Sci. Lett.* **359–360**, 219–226.
- Wells P. A. (1977) Pyroxene thermometry in simple and complex systems. *Contrib. Mineral. Petrol.* **62**, 129–139.
- Weyer S. and Ionov D. A. (2007) Partial melting and melt percolation in the mantle: the message from Fe isotopes. *Earth Planet. Sci. Lett.* **259**, 119–133.
- Wiechert U. and Halliday A. N. (2007) Non-chondritic magnesium and the origins of the inner terrestrial planets. *Earth Planet. Sci. Lett.* **256**, 360–371.
- Williams H. M. and Bizimis M. (2014) Iron isotope tracing of mantle heterogeneity within the source regions of oceanic basalts. *Earth Planet. Sci. Lett.* **404**, 396–407.
- Wu F.-Y., Walker R. J., Yang Y.-H., Yuan H.-L. and Yang J.-H. (2006) The chemical-temporal evolution of lithospheric mantle underlying the North China Craton. *Geochim. Cosmochim. Acta* **70**, 5013–5034.
- Xiao Y., Teng F.-Z., Zhang H.-F. and Yang W. (2013) Large magnesium isotope fractionation in peridotite xenoliths from eastern North China craton: product of melt–rock interaction. *Geochim. Cosmochim. Acta* **115**, 241–261.
- Yang W., Teng F.-Z. and Zhang H.-F. (2009) Chondritic magnesium isotopic composition of the terrestrial mantle: a case study of peridotite xenoliths from the North China craton. *Earth Planet. Sci. Lett.* **288**, 475–482.
- Young E. D. and Galy A. (2004) The isotope geochemistry and cosmochemistry of magnesium. *Rev. Mineral. Geochem.* **55**, 197–230.
- Young E. D., Tonui E., Manning C. E., Schauble E. and Macris C. A. (2009) Spinel-olivine magnesium isotope thermometry in the mantle and implications for the Mg isotopic composition of Earth. *Earth Planet. Sci. Lett.* **288**, 524–533.
- Zhong Y., Chen L.-H., Wang X.-J., Zhang G.-L., Xie L.-W. and Zeng G. (2017) Magnesium isotopic variation of oceanic island basalts generated by partial melting and crustal recycling. *Earth Planet. Sci. Lett.* **463**, 127–135.

Associate Editor: Nicolas Dauphas